

Proximity-coupled Ti/TiN multilayers for use in kinetic inductance detectors

Michael R. Vissers, Jiansong Gao, Martin Sandberg, Shannon M. Duff, David S. Wisbey, Kent D. Irwin, and David P. Pappas

Citation: *Applied Physics Letters* **102**, 232603 (2013); doi: 10.1063/1.4804286

View online: <http://dx.doi.org/10.1063/1.4804286>

View Table of Contents: <http://scitation.aip.org/content/aip/journal/apl/102/23?ver=pdfcov>

Published by the AIP Publishing

Articles you may be interested in

[Preparation of overdamped NbTiN Josephson junctions with bilayered Ti–TiN barriers](#)

J. Appl. Phys. **108**, 113904 (2010); 10.1063/1.3517475

[Proximity effects in asymmetric layered ferromagnet/superconductor nanostructures](#)

J. Appl. Phys. **105**, 07E128 (2009); 10.1063/1.3068423

[Nanoindentation investigation of Ti/TiN multilayers films](#)

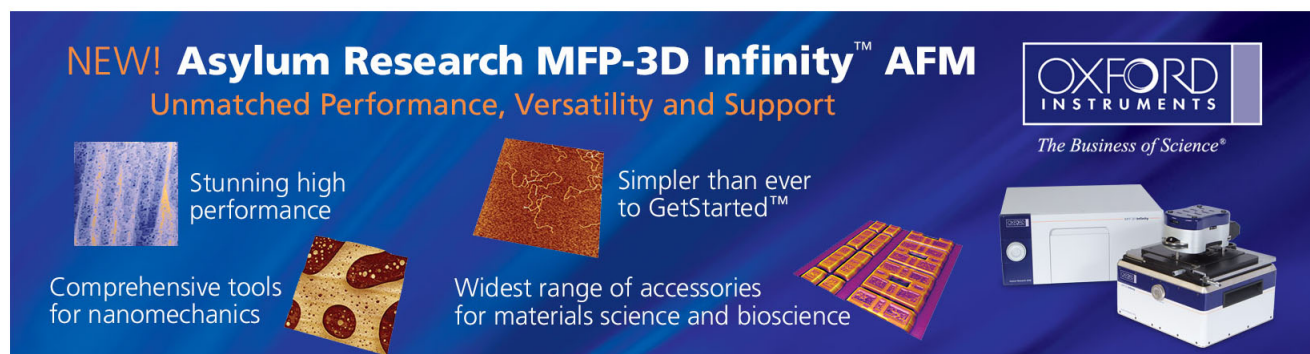
J. Appl. Phys. **87**, 7753 (2000); 10.1063/1.373450

[Properties of Ni/Nb magnetic/superconducting multilayers](#)

J. Vac. Sci. Technol. A **15**, 1774 (1997); 10.1116/1.580868

[Proximity and coupling effects in superconductor/ferromagnet multilayers \(invited\)](#)

J. Appl. Phys. **81**, 5358 (1997); 10.1063/1.364545

This is a promotional banner for the Asylum Research MFP-3D Infinity AFM. The background is dark blue. On the left, there are three small images: a blue textured surface, a brown textured surface, and a yellow and red patterned surface. To the right of these images are three text blocks: 'Stunning high performance', 'Simpler than ever to GetStarted™', and 'Widest range of accessories for materials science and bioscience'. Below the first two text blocks is a fourth text block: 'Comprehensive tools for nanomechanics'. On the far right, there is a large image of the AFM instrument, which is a white and blue box with a sample stage on top. Above the instrument is the Oxford Instruments logo, which consists of the word 'OXFORD' in a large, white, serif font and 'INSTRUMENTS' in a smaller, white, sans-serif font below it. Below the logo is the tagline 'The Business of Science®'.

Proximity-coupled Ti/TiN multilayers for use in kinetic inductance detectors

Michael R. Vissers,^{1,a)} Jiansong Gao,¹ Martin Sandberg,¹ Shannon M. Duff,¹
 David S. Wisbey,² Kent D. Irwin,¹ and David P. Pappas^{1,b)}

¹National Institute of Standards and Technology, 325 Broadway, Boulder, Colorado 80305, USA

²Department of Physics, Saint Louis University, 3450 Linden Blvd., Saint Louis, Missouri 63103, USA

(Received 21 September 2012; accepted 23 April 2013; published online 14 June 2013)

We apply the superconducting proximity effect in TiN/Ti multi-layer films to tune the critical temperature, T_C , to within 10 mK with high uniformity (less than 15 mK spread) across a 75 mm wafer. Reproducible T_C 's are obtained from 0.8 to 2.5 K. These films had high resistivities, $>100\mu\Omega\text{ cm}$, and internal quality factors for resonators in the GHz range, on the order of 100 k and higher. Trilayers of both TiN/Ti/TiN and thicker superlattice films were prepared, demonstrating a well controlled process for films over a wide thickness range. Detectors were fabricated and shown to have single photon resolution at 1550 nm. The high uniformity and controllability coupled with the high quality factor, kinetic inductance, and inertness of TiN make these films ideal for use in frequency multiplexed kinetic inductance detectors and potentially other applications such as nanowire detectors, transition edge sensors, and associated quantum information applications. © 2013 AIP Publishing LLC. [<http://dx.doi.org/10.1063/1.4804286>]

Microwave kinetic inductance detectors (MKIDs) development has been important over the past 10 years, for applications in astronomical instruments from sub-mm to gamma-ray¹ and non-astronomical applications.^{2,3} MKIDs are based on high Q resonators. The key advantage of MKIDs is that they can be easily frequency multiplexed and are relatively simple to fabricate from a single film. Use of the superconducting material titanium nitride (TiN) in particular for these devices has recently attracted attention because resonators fabricated from this material have high kinetic inductance, high normal resistivity, and very low loss for resonators in the GHz range.^{4,5} This low loss translates into a very high internal quality factor, Q_i , while the high kinetic inductance and resistivity greatly improve responsivity and facilitate optical coupling, respectively. Uniformity in these properties is therefore crucial for scaling up to large arrays of devices for astronomical applications. However, standard TiN growth methods do not yield the required sufficient uniformity in low T_C films for these important applications. In this work we present a different growth method utilizing TiN/Ti multilayers that greatly improves the uniformity while retaining the best properties of the TiN monolayers.

An important property of TiN is the tunability of the superconducting critical temperature, T_C , from 0 to 5 K, by adjusting the nitrogen concentration. This allows films made from various TiN_x compounds to be tailored for specific applications. For example, films with $T_C \sim 1$ K are the ideal choice for photon-counting MKIDs because the sensitivity improves as the T_C is lowered (frequency shift per photon $\delta f \propto 1/T_C^2$), while it is still high enough to prohibit thermal quasi-particle formation at the typical bath temperature of $T \sim 100$ mK. In addition, a T_C of 1 K is needed for mm-wave MKIDs used in cosmic microwave background (CMB) detection. The two most used CMB bands for ground-based instruments are 90 GHz and 150 GHz, which require T_C to be

below 1.2 K and 2 K, respectively, in order for the mm-wave photons to break Cooper-pairs in the superconductor.⁶ In fact, TiN with $T_C \sim 1$ K range is preferred for applications in the entire 90–300 GHz range.

Sub-stoichiometric TiN films with T_C around 1 K have been made into photon-counting detectors at UV/Optical/NIR wavelengths and have shown single photon sensitivity.^{7,8} However, it is difficult to control the targeted T_C in these sub-stoichiometric films; additionally, the films show large non-uniformity across the wafer.^{7,9,10} This is due to two compounding effects. First, T_C is a very strong function of the N content because the change in T_C occurs over a narrow range of N concentration, just above the Ti_2N phase.⁹ Second, it is difficult to maintain precise control of the nitrogen incorporation process from run-to-run and across large areas. This is due to the fact that N is introduced to the process as a flow of gas into a reactive sputtering chamber. Inside the chamber there is a complex interplay of gas flows, target voltages, and target erosion profiles. Using a standard UHV vacuum chamber with 75 mm sputter targets, variations on the order 500 mK between runs and across the wafer are typical.⁹ This difficulty in controlling T_C is a great challenge that must be solved before TiN can be used in large MKID arrays.

In this letter, we take a different approach. We use a multi-layer of pure Ti and stoichiometric TiN, exploiting the superconducting proximity effect to obtain the target T_C while maintaining the desirable qualities of the TiN at the surfaces and interfaces.^{11,12} This approach works well because it is comparatively easy to reproducibly grow layers of these materials that are homogeneous and have a constant thickness (within 5%) across the wafer. Titanium and TiN have T_C 's of 0.4 and 5 K, respectively, and by adjusting the relative thicknesses of these layers it is possible to tune the T_C between these two limiting values.

Theories to explain the superconducting proximity effect have been formulated since the first experiments were performed.¹³ The fundamental non-locality of superconductivity

^{a)}Electronic mail: michael.vissers@nist.gov

^{b)}Electronic mail: david.pappas@nist.gov

implies that for multi-layer thin films, T_C depends not only upon the intrinsic superconducting properties of the constituent materials but also on the interaction of the different layers. Cooper's early description¹⁴ of the proximity effect dealt with the T_C of a normal-superconducting bilayer where the thicknesses of the two layers were less than any relevant length scale. These same arguments can be extended to multi-layers.^{15–17} The T_C of these films is then determined by (1) the average of the T_C 's of the constituent parts weighted by the number of electrons contributed by each layer and (2) the spatial extent of the proximitization. For the superconductor, this scale is determined by the size of the Gor'kov kernel, which in dirty films is $\propto (\xi l)^{1/2}$,¹⁸ where ξ is the coherence length and l the electron mean free path. Specifically, for TiN we have measured the Ginzburg-Landau coherence length $\xi_{TiN} = 13 \pm 2$ nm (from measurements of H_{C2} vs. temperature) and l is on the order of the grain size, i.e., about 20 nm for these films. For the normal metal, i.e., Ti well above its superconducting transition temperature, the proximitization scales with the electron mean free path, which also is limited by the grain size.¹⁹ This sets the Ti and TiN film thicknesses of interest for this study to be up to about 20 nm.

We have chosen to create trilayer and superlattice structures with TiN at the top and bottom interfaces, e.g., TiN/Ti/.../TiN. This structure preserves the known good metal-vacuum and metal-Si interface properties of TiN films. More specifically, it suppresses oxidation by protecting the Ti film and may also reduce the surface and interface two level systems (TLS's) in the multilayers that are known to lead to frequency noise and dissipation in monolayer resonators.^{4,5} The non-locality of superconductivity implies that the trilayers and multi-layers will act functionally the same as the bilayer structure discussed above, with a single T_C for the entire film. The films were grown in a UHV sputter tool similar to that described previously.⁵ Figure 1(a) illustrates the heterostructure of the deposited film grown on high-resistivity Si wafers. The wafers were first cleaned in HF, immediately transferred to the growth chamber, and then heated to 500°C on a rotating platen. A short (60 s) preliminary soak was performed in Ar:N₂ with the shutters on the gun and at the sample closed and the gun and sample RF bias on. This soak serves to form a ≈ 1 nm layer of SiN that acts both as an insulator and as a buffer layer for subsequent growth of (200)-textured TiN. The buffer layer reduces the nucleation of the (111)-texture, which we have found deleterious for the RF properties of TiN.⁵ The first layer of stoichiometric TiN was deposited at high temperature by use of reactive sputtering in the Ar:N₂ mixture. In our chamber, we found that growing at elevated temperature resulted in stoichiometric TiN monolayers with the best RF performance.⁵ Hence, we chose to use the high temperature TiN for the bottom layer to utilize the best TiN-substrate interface. The N₂ partial pressure was stabilized using an upstream thermal mass flow controller and by throttling the chamber pump downstream. The sample was then cooled, and subsequent layers were grown at low (≈ 300 K) temperature to reduce any nitrogen diffusion. Between growths of the individual layers, the Ti sputter gun was run with both shutters closed and N₂ flow set either off or on to prepare the Ti target surface for the next layer. This

is important because during the TiN deposition the surface of the Ti sputter source becomes fully nitrided and must be cleaned in order to subsequently deposit pure Ti; after the Ti deposition the target is then re-nitrided.

The trilayer and superlattice films were then patterned into test structures for measurements of T_C , resonator quality factor, and detectors for photon counting at near infrared wavelengths. For all measurements the samples were cooled in an adiabatic demagnetization refrigerator (ADR) that has a base temperature of ≤ 100 mK and variable temperature control up to 10 K. Room temperature resistivities on the order of $100 \mu\Omega\text{cm}$ and a residual resistance ratio (RRR) of ~ 1 were measured. Superconducting critical temperature measurements were conducted at both DC and AC (at RF ≈ 4 GHz). As shown in Fig. 1(b), the DC transition from the normal to superconducting states is very sharp, with a width of less than 25 mK.

Figure 1(c) shows the measured superconducting transition at DC for films as a function of total TiN thickness, d , and Ti thicknesses, D . As expected, increasing the TiN thickness (or decreasing the Ti thickness) leads to an increased T_C . Furthermore, the heavier weighting of the more metallic Ti is evident because the measured T_C 's are less than a simple average would predict. We also observe a range of TiN thicknesses where T_C is relatively insensitive to the thicknesses of the constituent layers. This region, with $T_C \approx 1.3$ K and total TiN thickness between 5 and 10 nm, exhibits a significantly reduced slope in T_C vs TiN thickness. The origin of this effect is still under investigation, but we hypothesize that it is due to inter-facial effects and intermixing between the TiN and the Ti or other growth kinetics that do not scale with TiN thickness. The T_C scaling carries over to the thicker superlattice films. Figure 1(c) also shows a datum taken from a 3/10/3/10/3/10/3 nm TiN/Ti/TiN superlattice (star symbol). With $T_C = 1.4$ K, i.e., the same as the trilayers with similar Ti/TiN ratios, the superlattice illustrates the scalability of these multilayer devices. This result implies that films of almost arbitrary thickness can be grown, with the T_C controlled by the relative thicknesses of the TiN and Ti layers. In addition, we find that T_C for nominally identical films is reproducible within $\leq 2\%$.

To illustrate and compare the homogeneity of T_C for these multi-layer films on a given wafer relative to sub-stoichiometric films, we show the variation of T_C across a 75 mm wafer for both processes in Fig. 2. As shown in Fig. 2(a), the multi-layer films show less than 1.5% variation of T_C across the wafer (15 mK variation on a $T_C = 1$ K wafer). The wafer map shown in Fig. 2(b) illustrates that multi-layers are very homogeneous across the wafer, with only a slight radial dependence that is at the limit of the T_C measurement resolution. The reproducibility of T_C and better homogeneity across the wafer for the multi-layers is due to the fact that the absolute thickness of the Ti and TiN can be controlled precisely at the sub-nm level combined with the relative insensitivity of T_C to TiN thickness in this range. This is illustrated by the comparison of the measured resonances in Figure 2(e) of two nominally identical dies from the center and edge of a 3 in. TiN/Ti/TiN multilayer film. The resonances differ by less than 2%, indicating that the response of the TiN is uniform across the wafer.

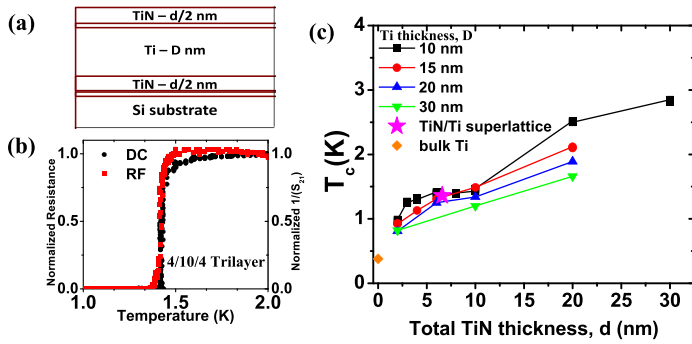


FIG. 1. (a) Schematic of a trilayer. (b) Measured resistance and $(S_{21} \text{ transmission})^{-1}$ versus temperature at DC and 6 GHz of a 4/10/4 nm Ti/TiN/Ti trilayer. (c) Measured T_C at DC of trilayers vs TiN thickness for various Ti thicknesses.

For comparison, Fig. 2(a) also shows that the T_C on a wafer with sub-stoichiometric TiN varies by more than 25%, and Fig. 2(c) illustrates that this non-uniformity has a strong radial dependence. A similar contrast is seen in Fig. 2(d) where the sheet resistance across the wafer is considerably greater for the sub-stoichiometric film. The non-uniformity in the sub-stoichiometric films is thought to be due to uneven nitrogen gas flow throughout the chamber. This nitrogen will unevenly react with unbonded Ti in the deposited film; the radial dependence is caused by the symmetry imposed by the rotation of the substrate during deposition. The extreme sensitivity of the TiN's T_C to the nitrogen flow means that small variations in the nitrogen concentrations due to gas loading and inhomogeneous flow in the chamber lead to variations of hundreds of mK in the T_{C_X} across the wafer.^{7,9,10}

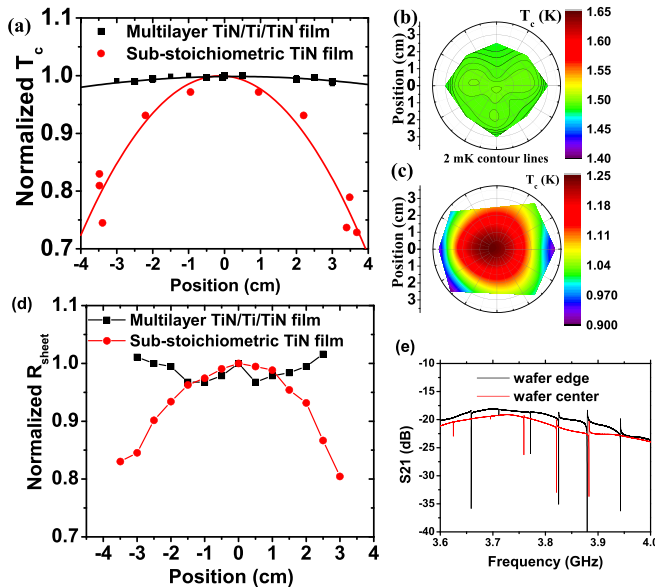


FIG. 2. (a) T_C vs position for the multi-layer stoichiometric TiN/Ti/TiN (black) and mono-layer (red) sub-stoichiometric TiN based thin films. The multi-layer has $10\times$ less variation in T_C . The lines are a guide to the eye. (b) and (c) Corresponding contour plots of measured T_C in stoichiometric multi-layer and sub-stoichiometric mono-layer wafers. (d) Normalized sheet resistance vs position for both a trilayer TiN/Ti/TiN film (black) and a sub-stoichiometric monolayer (red). The resistivity variation in the multi-layer is likely due to film thickness variations, while the nominally identical thickness variations in the sub-stoichiometric film is dominated by the compositional changes in resistivity.⁹ (e) Measured S_{21} vs frequency curves from separate center (red) and edge (black) dies. The resonances differ by ≤ 30 MHz or $\sim 1\%$. Known inhomogeneities in the etch resulting in deeper trenches in the resonator gaps near the edge of the wafer^{11,22} may also contribute to the variations in resonator frequency.

For RF measurements, the films were patterned into quarter-wave, co-planar waveguides (CPWs) and lumped-element, kinetic inductance detector (LEKID)-style resonators. The resonators were capacitively coupled to a CPW feed-line. We first measured the RF transmission through the feed-line near T_C . Figure 1(b) shows the transmission data from a device fabricated from a 4/10/4 nm TiN/Ti/TiN film with a $T_C = 1.4$ K. Since the film is much thinner than the penetration depths of the TiN (~ 300 nm) or Ti (~ 100 nm),⁵ the current should be distributed throughout the film thickness. Thus, the RF transmission is a good measure of the T_C of the entire film stack. For example, if the Ti layer in the center of the multi-layer was too thick, hence not completely proximitized, the RF transmission would not stop decreasing until the full multi-layer was superconducting. We measured a sharp S_{21} transition of the multi-layer at $T_C(\text{DC})$ with no other visible structure at low temperature. This indicates that the all of the layers of the film are fully proximitized.

We then performed standard resonator measurements at the ADR base temperature. The measured and derived properties for several resonators are listed in Table I. These include T_C at DC, Q_i , the penetration depth λ (extracted from the kinetic inductance-induced frequency shift fraction or the 4 K resistivity⁵), the normal state DC resistivity, ρ_n and the calculated kinetic sheet inductance, L_s . While the measured Q_i is less than that reported for stoichiometric TiN,^{4,5} the values for the multi-layers compare well with the measured sub-stoichiometric TiN film with a similar T_C . A general trend of decreasing Q_i is observed as T_C decreases. However, these numbers should still be high enough for applications in a MKID.

In order to directly test the efficacy of these multi-layers in an actual detector, we fabricated a photon counting MKID from a trilayer film with $T_C = 1.3$ K. The device design, experimental setup, measurement procedures, and data analysis are identical to our previous photon-counting experiment with sub-stoichiometric $T_C = 1.3$ K TiN LEKID.⁷ We use the photon-counting experiment as a tool to derive important properties of the trilayer TiN and to study its electrodynamics. Because the detector design is not optimized for 1550 nm light, it is not the focus of our paper here to demonstrate the best energy resolution. In spite of this, we still obtain single photon resolution in this range. Figure 3 shows a pulse height histogram from 10 000 laser pulses. The first 2 peaks are clearly resolved and correspond to the events of 0 and 1 photons being detected by the detector. From a 3-peak Gaussian fit we have extracted the energy resolving power $E/\Delta E = 0.6$ and the energy resolution $\Delta E = 0.48$ eV. The

TABLE I. Low temperature properties of RF resonators from TiN/Ti multi-layers and a sub-stoichiometric film. For films that were not patterned into resonators, no Q_i data are available, and penetration depths (marked with an asterisk) were calculated from the resistivity measured at 4 K. The kinetic sheet inductance is calculated from $L_s = \frac{\hbar \rho_s}{\pi \Delta_0 t}$, where Δ_0 is the BCS gap and t is the film thickness.²

Type	Film	T_C [K]	Q_i	λ [nm]	ρ_n [$\mu\Omega$ cm]	L_s [pH/sq]
CPW	Tri-layer 15/10/15	2.5		785*	100	14
CPW	Tri-layer 4/10/4	1.4	250 000	800	110	60
LEKID	Tri-layer 4/10/4	1.4	100 000	950	100	55
CPW	Superlattice 3/10/.../3	1.4		1010*	120	21
LEKID	Sub-stoichiometric	1.3	300 000	1000	100	53
CPW	Tri-layer 2/15/2	1.1	80 000	900	130	86
CPW	Tri-layer 1/20/1	0.8		1110*	90	71

recombination time was measured to be $50 \mu\text{s}$. These values are similar to that measured in the sub-stoichiometric film. Additionally, the resonance frequencies of both the monolayer and trilayer films are within 1%, illustrating the close similarities in kinetic inductance and other electrical properties of the two films. This is further supported by the fact that we have observed that the trilayer MKID used in this study also shows the same anomalous temperature and pulse response as reported earlier for detectors made from sub-stoichiometric TiN films. Therefore neither multilayer nor monolayer TiN films can be fully described by the standard Mattis-Bardeen theory. Furthermore, the multilayer structure may show additional physics due to proximity effects.²⁰ Further study is needed to understand the electrodynamics of these strongly disordered films,²¹ an important avenue of research for detector applications.

In conclusion, we have utilized TiN/Ti/TiN multi-layers to create highly uniform films on 75 mm Si wafers with fine control of the T_C for use as MKIDs and photon detectors. Compared to sub-stoichiometric films, the uniformity in T_C is substantially improved, with much greater reproducibility between wafers. The desirable properties of TiN, i.e., high resistivity and kinetic inductance, low RF loss and easy coupling to radiation due to the high resistivity of the material are found to be preserved. For MKID applications that would require a film thicker than 20 nm, the 10-layer superlattice increases the thickness to 60 nm. The trilayer MKID is sensitive to single photons at 1550 nm and has shown a similar energy resolution to its monolayer sub-stoichiometric counterpart. In addition, the 1.3 K TiN is another superconducting material that could offer a potential alternative to Al for some MKID applications. The fine control of T_C and the uniform response across the wafer would also be interesting for nanowires and transition edge sensors (TES). Furthermore, the ability of maintaining the low loss TLS interfaces implies that the range of high performance resonator devices could be extended to other astronomical and other applications.

We acknowledge support for this work from DARPA, the Keck Institute for Space Studies, the NIST Quantum Initiative, and NASA under Contract No. NNH11AR831.

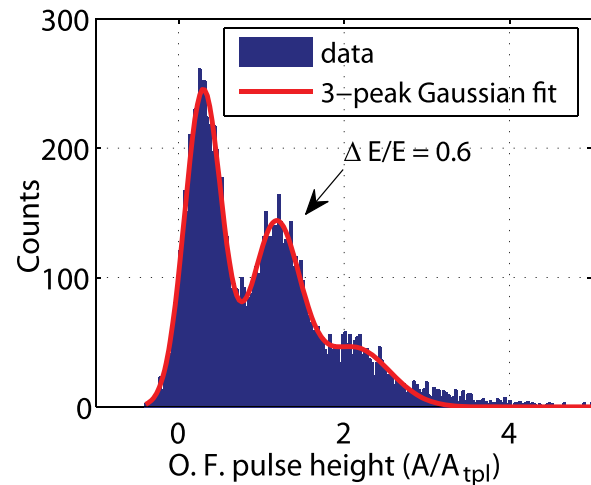


FIG. 3. Photon counting statistic of the 1.3 K trilayer LEKID in response to 1550 nm photons.

The authors thank Jonas Zmuidzinas, Henry Leduc, and Martin Weides for helpful discussions and insights.

- ¹P. Day, H. G. LeDuc, B. A. Mazin, A. Vayonakis, and J. Zmuidzinas, *Nature (London)* **425**, 817 (2003).
- ²J. Zmuidzinas, *Annu. Rev. Condens. Matter Phys.* **3**, 169 (2012).
- ³T. Cecil, A. Miceli, O. Quaranta, C. Liu, D. Rosenmann, S. McHugh, and B. Mazin, *Appl. Phys. Lett.* **101**, 032601 (2012).
- ⁴H. G. Leduc, B. Bumble, P. K. Day, B. H. Eom, J. Gao, S. Golwala, B. A. Mazin, S. McHugh, A. Merrill, D. C. Moore, O. Noroozian, A. D. Turner, and J. Zmuidzinas, *Appl. Phys. Lett.* **97**, 102509 (2010).
- ⁵M. R. Vissers, J. Gao, D. S. Wisbey, D. A. Hite, C. C. Tsuei, A. D. Corcoles, M. Steffen, and D. P. Pappas, *Appl. Phys. Lett.* **97**, 232509 (2010).
- ⁶B. Mazin, Ph.D. dissertation, California Institute of Technology, 2004.
- ⁷J. Gao, M. R. Vissers, M. O. Sandberg, F. C. S. da Silva, S. W. Nam, D. P. Pappas, D. S. Wisbey, E. C. Langman, S. R. Meeker, B. A. Mazin, H. G. Leduc, J. Zmuidzinas, and K. D. Irwin, *Appl. Phys. Lett.* **101**, 142602 (2012).
- ⁸S. McHugh, B. A. Mazin, B. Serfass, S. Meeker, K. O'Brien, R. Duan, R. Raffanti, and D. Werthimer, *Rev. Sci. Instrum.* **83**, 044702 (2012).
- ⁹M. R. Vissers, J. Gao, J. S. Kline, M. Sandberg, M. Weides, D. S. Wisbey, and D. P. Pappas, *Thin Solid Films*, e-print [arXiv:1209.4626](https://arxiv.org/abs/1209.4626).
- ¹⁰P. Diener, H. Leduc, S. J. C. Yates, Y. J. Y. Lankwarden, and J. J. A. Baselmans, *J. Low Temp. Phys.* **167**, 305 (2012).
- ¹¹M. Sandberg, M. Vissers, J. S. Kline, M. Weides, J. Gao, D. S. Wisbey, and D. P. Pappas, *Appl. Phys. Lett.* **100**, 262605 (2012).
- ¹²J. Wenner, R. Barends, R. C. Bialczak, Yu Chen, J. Kelly, E. Lucero, M. Mariantoni, A. Megrant, P. J. J. Malley, D. Sank, A. Vainsencher, H. Wang, T. C. White, Y. Yin, J. Zhao, A. N. Cleland, and J. M. Martinis, *Appl. Phys. Lett.* **99**, 113513 (2011).
- ¹³H. Meissner, *Phys. Rev.* **117**, 672 (1960).
- ¹⁴L. Cooper, *Phys. Rev. Lett.* **6**, 689 (1961).
- ¹⁵N. Sato, *J. Appl. Phys.* **67**, 7493 (1990).
- ¹⁶G. Ventura, M. Barucci, E. Pasca, E. Monticone, and M. Ratjeri, in *Proceedings of 7th International Conference on Advanced Technology and Particle Physics*, 2002, p. 677.
- ¹⁷A. Luukanen, H. Sipila, K. Kinnunen, A. Nuottajarvi, and J. Pekola, *Physica B* **284–288**, 2133 (2000).
- ¹⁸J. R. Waldram, *Superconductivity of Metals and Cuprates* (IOP Publishing, London, 1996).
- ¹⁹C. Reale, *Rev. Bras. Fis.* **3**(3), 431 (1973).
- ²⁰S. Zhu, T. Zijlstra, A. A. Golubov, M. van den Beemt, A. M. Baryshev, and T. M. Klapwijk, *Appl. Phys. Lett.* **95**, 253502 (2009).
- ²¹E. F. C. Driessen, P. C. J. J. Coumou, R. R. Tromp, P. J. de Visser, and T. M. Klapwijk, *Phys. Rev. Lett.* **109**, 107003 (2012).
- ²²M. R. Vissers, J. S. Kline, J. Gao, D. S. Wisbey, and D. P. Pappas, *Appl. Phys. Lett.* **100**, 082602 (2012).